ACS OMEGA

Open Access

http://pubs.acs.org/journal/acsodf

Article

Pilot-Scale Experimental Investigation on Dry Capture of Mercury and SO_3 in Smelting Gas of Acid Making

Wei Liu,[#] Xin Min,[#] Jin Zhao, and Songjian Zhao*

Cite This: *ACS Omega* 2023, 8, 42741−42747

Read Online

ACCESS | Metrics & More | Article Recommendations | Supporting Information

ABSTRACT: In this study, a novel dry capture process utilizing a mixed adsorbent of ZnO and CuS was proposed for the simultaneous removal of Hg^0 and SO_3 in flue gas from zinc smelting, addressing severe mercury pollution and high SO_3 concentrations. The experimental results showed that flue gas cooling caused the SO_3 to transform into sulfuric acid mist, which changed the reaction mechanism from a gas−solid to a liquid−solid reaction and helped to improve the SO_3 removal efficiency. Additionally, properly increasing the absorbent/SO_3 molar ratio significantly improved the SO_3 removal performance. However, excessive absorbent injection could cause aggregation and uneven dispersion of the absorbent particles in the flue gas, therefore impairing the effectiveness of SO_3 capture. Under typical operating conditions (flue gas flow rate of 3500 m^3/h, flue gas temperature of 180 °C, ZnO/SO_3 molar ratio of 0.74, and residence time of 0.5 s), using a mixed absorbent of ZnO and CuS achieved an SO_3 removal efficiency of up to 32.6%, and a total mercury capture at 43.2%, of which the Hg^0 removal attained a remarkable 76.3%. These results preliminarily confirm the feasibility of the dry capture technology for simultaneous removal of SO_3 and mercury, laying the foundation for further application and promotion.

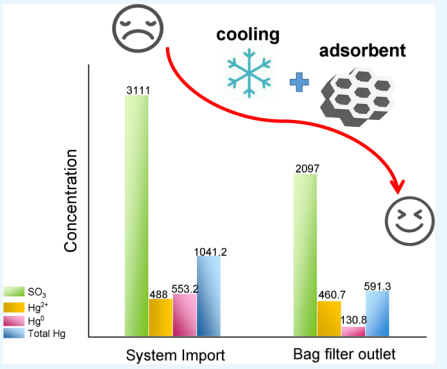

1. INTRODUCTION

As China has become the world's largest producer of zinc ore, the rapid growth and expansion of the zinc industry has caused serious impacts and damage to the local ecological environment, including air pollution, water and soil erosion, and soil contamination.[1,2] These environmental concerns need to be addressed, as they not only threaten the health and well-being of local residents, but also have implications for broader environmental and public health issues.[3] During the zinc extraction process, mercury tends to coenrich with zinc sulfide ore, resulting in a distinctive composition of high-temperature flue gas during roasting.[4−6] After the mixture is subjected to waste heat recovery and dust removal treatment, the composition of the high-temperature flue gas from the roasting process changes. Sulfur dioxide (SO_2) becomes its predominant component, though it also contains high concentrations of both mercury and sulfur trioxide (SO_3) pollutants. Although existing dust removal equipment can effectively remove most particulate mercury (Hg^p), the capture efficacy of elemental mercury (Hg^0) is relatively poor. This results in a substantial amount of mercury transferring to acid wastewater during the washing and degassing process, making acid wastewater treatment much more challenging.[7,8] Therefore, the investigation of mercury pollution control technologies for zinc mining is of paramount practical significance.

Currently, the control technologies for high-concentration mercury in smelting flue gas mainly fall into two categories: (1) dedicated mercury removal technologies, mainly including adsorption filtration and chemical absorption. Adsorption filtration technologies such as charcoal filters and selenium filters have been eliminated due to their low filtration efficiency and toxicity.[9,10] Chemical absorption technologies, represented by mercury chloride absorption processes, are currently the most mature technologies applied in nonferrous smelters. However, this technology is outdated and has not seen recent developments due to its higher costs, complex operation, and risks of secondary pollution. Currently, only a small number of smelters, such as Hunan Zhuzhou Smelter Group Co., Ltd., are equipped with mercury chloride removal facilities, but they have been abandoned in their new relocation project. (2) Coordinated control using existing pollution control devices, mainly including dust removal units, wet scrubbers, and electrostatic precipitators.[11,12] Currently, the main method of mercury pollution control measures in China's smelting industry is coordinated mercury removal. The coordinated capture efficiency of pollution control equipment (including acid gas exhaust) for mercury ranges from 6.0 to 99.9%, but more than 95% of the mercury flows into waste residue, acid

Received: July 29, 2023
Revised: October 13, 2023
Accepted: October 16, 2023
Published: November 1, 2023

wastewater, and sulfuric acid, causing serious harm. Wet scrubbing and electrostatic precipitation are currently used in combination for controlling SO_3 in smelting flue gas, producing a large amount of acid wastewater in the power wave, cooling tower, and electrostatic precipitation processes as the main source of acidic heavy metal wastewater in smelters.[13] In summary, the current methods for controlling high-concentration mercury pollution are unable to meet the existing emission requirements and cannot effectively solve the problem of acid pollution caused by mercury and SO_3 in flue gas, as well as the problem of multimedium composite pollution easily caused by mercury in the process of transferring from process equipment.

The use of a sorbent injection system to induce adsorption of Hg^0, forming Hg^p, and then capturing it along with dust by the dust removal equipment, is considered the most promising mercury removal technology due to its simple process, convenient operation, and minimal secondary pollution.[14−16] Combining the high-concentration mercury pollution characteristics of flue gas and typical nonferrous metallurgical process flows, if dry precapture of high-concentration Hg^0 and SO_3 can be carried out prior to scrubbing and cooling, the problem of heavy metal mercury pollution and excessive acid pollution can be potentially addressed. Liu et al.[17] proposed that graphene-based bimetallic catalysts ((Fe, Co)@N-GN) can adsorb and remove Hg^0 and SO_3, but the preparation process is complicated and the cost is not suitable for practical factory applications. Currently, there is limited research on SO_3 sorbents in smelting flue gas, and only few reports on Hg^0 and SO_3 coadsorption materials have been found. Our previous work focused on the control of mercury pollution, and we studied the preparation of efficient mercury removal materials based on zinc smelting raw material sphalerite (ZnS) and developed a series of mercury adsorbents with high adsorption capacity, fast adsorption rate, and recyclability, such as Cu^{2+} activated ZnS to recover mercury,[18] using zinc concentrate to capture mercury in zinc smelting flue gas.[19] Copper sulfide (CuS) contains abundant Cu^{2+} and S_2^{2-} active sites, which can effectively stabilize Hg^0 on the material surface in the form of HgS and have a large mercury adsorption capacity (up to 50.17 mg/g (50% breakthrough)).[20] Therefore, the use of copper-based sulfide as a mercury sorbent is feasible. In previous studies, it was found that ZnO has a high selectivity for SO_3,[21] so the use of ZnO for selective absorption of SO_3 in flue gas is proposed as a control technology for zinc smelting flue gas. The zinc smelting process generates zinc calcine and zinc oxide intermediate products containing ZnO as the main component. The absorbed product, $ZnSO_4$, can be directly sent to the electrolysis process as a supplement for the leaching solution, making the use of this intermediate product as an absorbent more economical and convenient.

In this work, a remediation strategy that involves precapturing mercury and SO_3 using dry capture technology before wet scrubbing was proposed to address the challenges of mercury pollution and excessive acidic emissions in zinc smelting. In particular, this work constructs a dry capture technology for Hg/SO_3, which employs methods such as cooling and adsorption. A pilot test facility is built to verify the effectiveness of Hg/SO_3 dry capture technology in purifying high-temperature acid-making flue gas. This research aims to establish a foundation for the promotion and application of Hg/SO_3 dry capture technology in the future.

2. EXPERIMENTAL SECTION

2.1. Experimental Apparatus. The SO_3 and Hg^0 adsorption performance evaluation system, as shown in Figure 1, consists of several parts, including a gas flow control system,

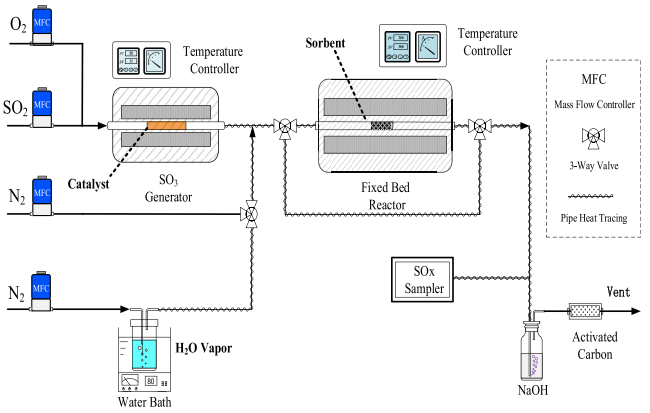

Figure 1. Flow diagram for SO_3 removal performance assessment.

SO_3 generator, Hg^0 generating device, fixed bed reaction system, SO_3 sampling system, mercury online detection device, and tail gas treatment system. Industrial V_2O_5/silica catalyst was used to catalyze the oxidation of SO_2 to SO_3. An appropriate amount of catalyst was packed into a quartz tube, and the SO_2 was almost completely catalytically oxidized to the SO_3 at a suitable reaction temperature. Hg^0 evaporates at high temperature through a mercury permeation tube, and then enters the testing atmosphere through N_2 blowing. The inner diameter and length of the quartz tube used in the experiment were 9 and 50 mm, respectively, and the catalytic reaction temperature was 480 °C. All gas pipelines and joints that came into contact with SO_3 and Hg^0 were made of PTFE material. To prevent SO_3 and Hg^0 from condensing, the outlet pipeline of the reaction furnace was equipped with an electric heat tracing tape for heat preservation with a heat tracing temperature of 200 °C.

2.2. Pilot-Scale Process and Equipment. The pilot-scale experimental apparatus was established following the sulfuric acid section of the production line in the first phase of a zinc smelting facility, which generated fume at a volume of approximately 60,000 m^3/h. The fume purification system in the sulfuric acid section consisted of several purification units including an electrostatic precipitator, dynamic wave scrubber, cooling bed, and electrostatic mist eliminator. The gas for the pilot experiment was sourced from the electrostatic precipitator following the roasting fume and controlled at a gas flow rate of 4000 m^3/h, temperature of 280 °C, moisture content of approximately 6.0%, O_2 content of approximately 7.4%, SO_2 concentration of approximately 8−9%, and SO_3 concentration of approximately 0.3%.

As illustrated in Figure S1, the entire experimental system mainly consisted of a forced draft fan, a primary heat exchanger, a cyclone dust collector, a secondary heat exchanger, a bag filter, and an absorbent injection device. The main principle of the technology was to reduce the flue gas temperature to near the acid dew point to cause condensation of SO_3 and formation of acid mist. High-concentration absorbent particles were injected into the flue gas, which provided favorable conditions for the adsorption of sulfuric acid mist due to their large specific surface area. Part of

https://doi.org/10.1021/acsomega.3c05443
ACS Omega 2023, 8, 42741−42747

Table 1. Equipment List

no.	designation	technical parameter	quantity	material
1	double eccentric hard-sealed butterfly valve	DN500, with high temperature and corrosion resistance	2	2507
2	system inlet flue	φ500	1	carbon steel
3	system outlet flue	φ300	1	304
4	induced draft fan	9−19−5.6 A/18.5 kW, flow rate of 4000−4900 m^3/h, pressure of 6954−6400 Pa	1	316L
5	first heat exchanger	self-made equipment	1	304
6	secondary heat exchanger	self-made equipment	1	304
7	heat exchange fan	flow rate of 5527−7700 m^3/h, pressure of 500−735 Pa	2	carbon steel
8	cyclone dust collector	Self-made equipment, designed airflow of 3000 N m^3/h	1	304
9	bag filter	DMC-112A, with an airflow of 3000 N m^3/h	1	carbon steel
10	metering screw feeder	DLX-63 × 0.4, with a motor power of 0.75 kW (Variant motors), conveying capacity of 0−50 kg/h	1	304
11	adsorbent injection system	Venturi, self-made	1	304

the acid mist was neutralized by alkaline substances, while the remainder was removed with dust in the bag filter. By mixing mercury and SO_3 absorbents and spraying them into the flue, we simultaneously adsorbed mercury and SO_3 were simultaneously adsorbed. All equipment and pipelines were insulated with 100 mm thick quartz wool to prevent SO_3 condensation and corrosion of the pipes and equipment.

Table 1 represents the inventory of pilot-scale experimental equipment. Considering the high temperature, corrosive nature, and resistance of fumes, stainless steel centrifugal fans were chosen to introduce fumes into the system. A variable frequency drive was also installed for flow regulation. The bag filter type DMC-112A, with a filtration area of 100 m^2, was equipped with PTFE filter bags that can withstand temperatures of up to 200 °C and 316 L bag cages. The equipment's resistance was ≤1.2 kPa. Its structure consists of a filter chamber, filter bags, clean air chamber, ash bin, ash discharge valve, pulse jet device, and electrical control box. The entire structure was made with a welding unit, and the inspection door was fitted with a foam rubber seal to ensure air tightness. The aim of installing a heat exchanger was to lower the fume temperature to near the acid dew point temperature. A tube-type heat exchanger was used, with air as the heat transfer medium, and two heat exchangers were installed, each with a matching blower. The heat transfer tubes were made of enamel that is resistant to high temperatures and corrosion. All materials in direct contact with the fumes were made of 304 stainless steel. Based on the on-site test results, the heat exchanger achieved satisfactory cooling performance. A cyclone separator was installed after the first-stage heat exchanger to separate particulate matter, prolong solid−gas reaction time, and reduce the load on the bag filter. The principle of cyclone separation relies on introducing tangential airflow to cause rotational movement, sending solid particles or liquid drops that have large inertia centrifugally outward to be separated from the airflow. The cyclone separator's main features include simple structure, high operational flexibility and efficiency, easy maintenance, and low price, and it captures dust with a diameter of 5−10 μm or larger. The cyclone separator's dust removal efficiency was designed to be >80%, and it was made with 304 stainless steel and equipped with an ash discharge valve.

2.3. Adsorbent Materials. The three adsorbent materials used in the experiments were ZnO, $CaCO_3$, and CuS. ZnO and $CaCO_3$ were of industrial grade. Cu $(NO_3)_2$ and Na_2S were dissolved, mixed at a molar ratio of 1:1, and aged after vigorous stirring. After aging, it was washed with deionized water, and then the sample was vacuum-dried and collected to obtain CuS. The purity, particle size, specific surface area, pore volume, and pore size of each adsorbent material were characterized and are presented in Table 2.

Table 2. Basic Parameters of Adsorbent Materials

category	purity	particle size μm	specific surface area m^2/g	pore volume m^3/g	pore size nm
ZnO	98%	6.62	2.282	3.638×10^{-3}	6.377
$CaCO_3$	98%	23.15	1.533	2.921×10^{-3}	6.998
CuS	99%	60.52	31.129	0.153	17.918

2.4. Experimental Procedures. The experiment aimed to investigate the synchronized capture of mercury and SO_3 by the pilot-scale test system under actual flue gas conditions. First, it studied the effect of stepwise cooling on SO_3 purification efficiency under high-temperature conditions followed by the exploration of the influence of sorbent type and dosage on SO_3 purification efficiency and the effectiveness of simultaneous removal of mercury and SO_3. In the experiment, the absorbent was injected into the flue gas duct from the outlet of the first heat exchanger to enable contact and reaction with the flue gas, leading to the removal of the SO_3 and mercury. The solid material leaving the reactor was collected by a dust collector. The concentrations of SO_3 and mercury in the inlet and outlet flue gas were analyzed and recorded based on the flue gas sampling results, to examine the removal efficiency of SO_3 and mercury before and after the absorbent was introduced.

2.5. Analytical Testing Methods. The improved EPA Method 29 uses two 0.05 mol/L NaOH solution absorption bottles (to absorb SO_2 and Hg^{2+} simultaneously), two 1 mol/L KCl solution absorption bottles (to absorb Hg^{2+}), and two 10% HNO_3−H_2O_2 absorption bottles (to absorb Hg^0) followed by two 4% $KMnO_4$-10% H_2SO_4 solution absorption bottles (to absorb Hg^0). Each absorption bottle is filled with 50 mL of solution, and the sampling is conducted at a gas flow rate of 1 L/min based on the experimental flue gas conditions. After the sampling of flue gas is completed, the same absorption solution is poured into a corresponding 500 mL volumetric flask. The flask and other glassware are washed with 5% HNO_3 three times, the washing liquid and the absorption solution are mixed, shaken well, and made up to volume. The concentration of mercury in the flue gas is measured by using a Lumex RA 915+ mercury analyzer and RP-91 accessory (detection limit 0.5 ng/L). The concentration of mercury in

https://doi.org/10.1021/acsomega.3c05443
ACS Omega 2023, 8, 42741−42747

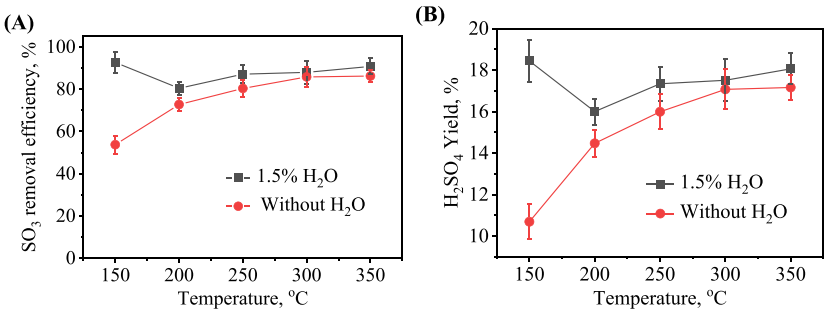

Figure 2. Temperature profiles of (A) SO_3 removal efficiency and (B) H_2SO_4 yield (reaction condition: 400 mL/min, 218 mg ZnO, 10% O_2, 500 ppm of SO_3).

the flue gas is calculated by determining the sampling flow rate and the sampling time. The cotton plug method is commonly used in the sulfuric acid industry for detection. The principle is that SO_3 in the gas is wetted by water in the cotton plug, which is converted into acid mist particles and filtered down. The acid mist trapped by the cotton plug is dissolved in water, and then, the SO_2 absorbed by the cotton plug is titrated with a standard iodine solution followed by titrating the total acid with a standard sodium hydroxide solution. The content of SO_3 is calculated based on the volume of the standard solution consumed during titration and the sampling volume of flue gas. The removal efficiencies of SO_3 (X_{SO_3}) and mercury (X_{Hg}) were calculated by the following formula:

$$X_{so_3} = \frac{(C_{SO_3})_{in} - (C_{SO_3})_{out}}{(C_{SO_3})_{in}} \times 100\%$$

$$X_{Hg} = \frac{(C_{Hg})_{in} - (C_{Hg})_{out}}{(C_{Hg})_{in}} \times 100\%$$

in which $(C_{SO_3})_{in}$ and $(C_{SO_3})_{out}$, $(C_{Hg})_{in}$ and $(C_{Hg})_{out}$ are denoted as the inlet and outlet molar concentration of SO_3 (mol/m^3), and the inlet and outlet molar concentration of mercury (mol/m^3) in steady-state conditions, respectively.

3. RESULTS AND DISCUSSION

3.1. Effect of Water Vapor on the Absorption Performance of SO_3. Initially, the impact of H_2O on the adsorption of SO_2 by ZnO was investigated, revealing minimal absorption of SO_2 by ZnO when the flue gas contained 10% H_2O (as shown in Figure S2). Furthermore, an investigation was conducted on the effect of water vapor on the adsorption of SO_3 by ZnO, where the reaction temperature and its impact on the adsorption efficiency and H_2SO_4 yield are represented in curves, as demonstrated in Figure 2A,B, respectively. Under dry conditions, the adsorption efficiency of ZnO for SO_3 increased monotonically with temperature, from 53.7% at 150 °C to 85.8% at 300 °C, and remained mostly consistent at 350 °C. Introducing H_2O enhanced the efficiency of ZnO to adsorb SO_3, particularly at lower temperatures. The most favorable adsorption efficiency of ZnO for SO_3, at 92.7%, was obtained under a water vapor content level of 1.5% and a temperature of 150 °C. Consistently, the conversion rate of SO_3 with respect to the temperature variation closely followed the same pattern as the adsorption efficiency. At a water vapor content level of 1.5% and a temperature of 150 °C, the conversion rate of SO_3 reached its maximum value of 18.4%.

H_2SO_4 is produced by the combination of SO_3 and water vapor in the flue gas. When the temperature of the flue gas drops to a certain value, H_2SO_4 begins to condense, and this temperature is called the acid dew point of the flue gas. The acid dew point temperature of the flue gas depends mainly on the content of SO_3 and water vapor and is calculated using the following formula:

$$T_{ld} = 186 + 20\lg V_{H_2O} + 26\lg V_{SO_3} \quad (1)$$

where V_{H_2O} is the volume fraction of water vapor in the flue gas, %; V_{SO_3} is the volume fraction of SO_3 in the flue gas, %; T_{ld} is the acid dew point temperature, °C. Based on the above formula, the acid dew point temperature of the flue gas in the present study is calculated to be 189.3 °C. Hence, H_2SO_4 exists in a gaseous state when the temperature is above 200 °C. At a temperature of 150 °C, which is below the dew point temperature of sulfuric acid, gaseous H_2SO_4 is converted into acid mist droplets. This process increases the vulnerability of the catalyst to adsorption by ZnO.

3.2. Effect of Flue Gas Cooling on SO_3 Concentration and Heat Recovery. As the flue gas temperature gradually decreases, gaseous SO_3 is first converted to gaseous H_2SO_4, and ultimately exists in the form of sulfuric acid droplets. The reactions with absorbent particles transition from a low-rate gas−solid reaction to a higher-rate gas−liquid reaction. Thus, changes in the flue gas temperature have a significant effect on SO_3 adsorption in the system. From Figure 3, with the heat

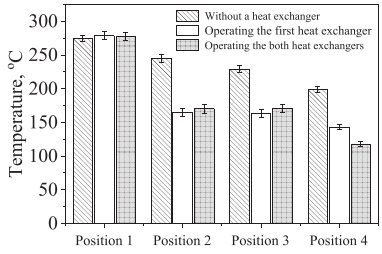

Figure 3. Temperature of flue gas before and after passing through the heat exchanger (positions 1 and 3 refer to the inlet of first and secondary heat exchangers, while positions 2 and 4 refer to the outlet of first and secondary heat exchangers, respectively).

exchange fan closed, the system's inlet temperature is 274.6 °C. After passing through the first heat exchanger, the temperature drops to 245 °C. Due to pipeline and cyclone separator heat dissipation, the temperatures at the inlet and outlet of the secondary heat exchanger are 228.9 and 198.6 °C, respectively. Without turning on the fan, the temperature difference before

https://doi.org/10.1021/acsomega.3c05443
ACS Omega 2023, 8, 42741−42747

and after the secondary heat exchanger is negligible. However, turning on the first heat exchanger causes the flue gas temperature to decrease rapidly from 278.8 to 165 °C, while the difference before and after the secondary heat exchanger remains small. Finally, with both heat exchange fans turned on, before-and-after-temperature differences of 277.4 and 170.9 °C, respectively, are recorded for the primary heat exchanger, and 170.7 and 117.8 °C, for the secondary heat exchanger, indicating excellent heat-exchanging performance and achieving the design value for the heat exchangers.

Figure 4 illustrates the variations of the SO_3 concentration at different flue gas temperatures. It can be found that when the

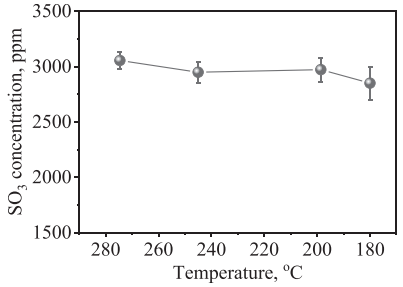

Figure 4. Effect of temperature on SO_3 concentration.

flue gas temperature is above 200 °C the SO_3 concentration remains relatively stable. However, when the temperature drops to 180 °C, a clear downward trend of the SO_3 concentration is observed, which could be attributed to the temperature being lower than the acid dew point, causing some SO_3 to condense and leading to a decrease in concentration.

3.3. Effect of Flue Gas Temperature on SO_3 Removal Efficiency. Further investigation was conducted to study the impact of flue gas cooling on the sorption performance of sorbents for SO_3 under the actual flue gas conditions. To avoid SO_3 condensation and bag blockage, the experiment was conducted under short-circuit conditions of the bag filter, where the sorbent was injected into the flue gas at the outlet of the first heat exchanger. The reaction between the sorbent and flue gas was then captured by the cyclone dust collector. Figure 5 shows that at a sorbent/SO_3 molar ratio of 0.37 and a

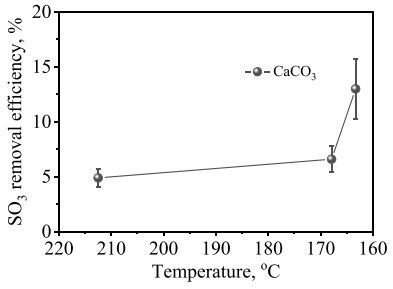

Figure 5. Effect of flue gas temperature on SO_3 removal efficiency (n_{CaCO_3}/n_{SO_3}= 0.37).

temperature of 212.5 °C, the SO_3 removal efficiency was only 4.9%. However, as the temperature decreased to 167.9 and 163.3 °C, the SO_3 removal efficiency increased to 6.6 and 13%, respectively. Comparing the pilot-scale experiment was compared with the fixed-bed reaction under laboratory conditions, the efficiency of the pilot-scale experiment was much lower. This is mainly attributed to the higher sorbent/SO_3 molar ratio of over 5 in the fixed-bed experiment that led to more efficient contact between the sorbent and SO_3. In contrast, the pilot-scale experiment was affected by multiple factors, such as sorbent concentration, the dispersion state of the sorbent in the flue gas, SO_3 concentration fluctuations, and reaction time, which resulted in poor SO_3 removal efficiency. However, a consistent rule was found that the SO_3 removal efficiency increased as the flue gas temperature decreased. Particularly, the efficiency increased significantly when the temperature was lower than the dew point temperature, indicating a transformation of gaseous SO_3 into sulfuric acid droplets and a change in the reaction mechanism from a gas−solid reaction to a liquid−solid reaction.[22]

3.4. Effect of Adsorbent Type and Dosage on SO_3 Removal Efficiency. The impact of the type and dosage of adsorbent on the removal efficiency of SO_3 was further studied under the condition of short-circuiting in a bag filter. As shown in Figure 6, the SO_3 removal efficiency of ZnO was

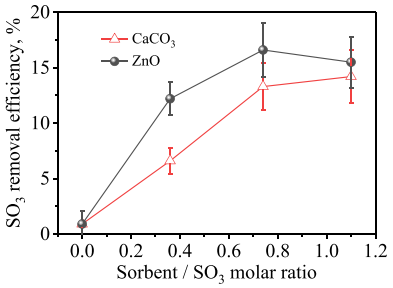

Figure 6. Effects of different sorbents and additions on the SO_3 removal efficiency.

significantly higher than that of $CaCO_3$, which is consistent with the results of laboratory fixed-bed experiments. When the absorber dosage/SO_3 molar ratio was 0.36, the SO_3 removal efficiencies for ZnO and $CaCO_3$ were 12.2 and 6.6%, respectively. When the dosage was doubled, the SO_3 removal efficiencies increased to 16.6 and 13.3%, respectively. However, further increasing the absorber dosage did not significantly enhance the SO_3 removal efficiencies, which were only 15.5 and 14.2%, respectively. The low utilization efficiency of the adsorbent may be because the adsorbent injected into the flue gas only has a transient contact with the gas before being captured by the cyclone separator, resulting in an inadequate reaction time (0.38 s).

3.5. Effect of the Simultaneous Removal of SO_3 and Mercury. Based on the actual situation of smelting flue gas and the optimal operating conditions determined from the above experiments, a pilot-scale test was conducted to simultaneously remove SO_3 and mercury using a composite adsorbent prepared with ZnO and CuS. The operating conditions and parameters of the pilot-scale experiment are shown in Table 3. Additionally, the concentrations of SO_3 and mercury at the specific positions after adding compound absorbent are presented in Table 4.

Under typical operating conditions, the average SO_3 removal efficiency using the composite adsorbent reached 32.6%, while the total mercury removal efficiency was 43.2%. The removal efficiency of Hg^0 was as high as 76.3%, which indicates that the pilot-scale experiment results could effectively verify the feasibility of the mercury/SO_3 dry capture technology.

https://doi.org/10.1021/acsomega.3c05443
ACS Omega 2023, 8, 42741−42747

Table 3. Experimental Operating Conditions for Simultaneous Removal of SO_3 and Mercury

indicators	parameters
flue gas flow rate (m^3/h)	3500
absorbent/SO_3 molar ratio	0.74
residence time (s)	0.5
absorbent	a mixture of 27.2 kg/h ZnO and 8.4 kg/h CuS
inlet temperature of first heat exchanger	277 °C
outlet temperature of first heat exchanger	178 °C
inlet temperature of secondary heat exchanger	180 °C
outlet temperature of secondary heat exchanger	156 °C

Due to the short residence time of the absorbent in the flue gas (only 0.5 s) and the lack of absorbent recirculation, the utilization rate of ZnO was low, resulting in a final ZnO conversion rate of approximately 13%. The absorbent byproduct was a dry mixture mainly composed of unreacted ZnO, with the remaining components consisting of $ZnSO_4$ and CuS adsorbed with mercury. These dry byproducts have stable chemical properties and would not cause secondary pollution to the environment. As the main component of the absorbent byproduct is ZnO, it cannot be directly sent to the leaching process. Therefore, a thermal treatment can be performed to recover desorbed high-concentration Hg^0, followed by sending the byproduct to a boiling furnace or volatilization kiln for further calcination to recover ZnO.

4. CONCLUSIONS

This study investigated a new method of using ZnO to recover SO_3 based on the characteristics of the zinc sulfide smelting process. By integration of the research results, a pilot study was carried out on the Hg^0/SO_3 dry capture technology for acid gas flue gas. In the pilot system, a mixed spray of mercury adsorbent and SO_3 absorbent was used to capture different pollutants with different functions of adsorbent, achieving the simultaneous removal of both pollutants in one system. The experimental results preliminarily verified the feasibility of the dry capture of mercury and simultaneous removal of the SO_3 technology, laying the foundation for further promotion and application. The main conclusions are as follows:

Lowering the flue gas temperature helps to improve the SO_3 removal efficiency. When the $CaCO_3/SO_3$ molar ratio was 0.37, the SO_3 removal efficiency was only 4.9% at a higher temperature of 212.5 °C. When the temperature was lowered to 167.9 °C, the SO_3 removal efficiency increased to 6.6%. When the temperature was further lowered to 163.3 °C, the removal efficiency significantly increased to 13%. The lower temperature causes SO_3 to transform into sulfuric acid mist, changing the reaction mechanism from a gas−solid reaction to a liquid−solid reaction and improving the reaction rate.

Increasing the absorbent/SO_3 molar ratio appropriately can significantly improve the SO_3 removal efficiency. When the absorbent/SO_3 molar ratio was 0.36, using ZnO and $CaCO_3$ as absorbents resulted in SO_3 removal efficiencies of 12.2 and 6.6%, respectively. When the absorbent/SO_3 molar ratio was 0.74, the SO_3 removal efficiencies were 16.6 and 13.3%, respectively. When the absorbent/SO_3 molar ratio increased to 1.1, the SO_3 removal efficiencies hardly increased, and were 15.5 and 14.2%, respectively. This is because excessive absorbent injection can cause agglomeration, resulting in uneven dispersion of absorbent particles in the flue gas and affecting the SO_3 removal efficiency.

■ ASSOCIATED CONTENT

Data Availability Statement

All data and materials generated or analyzed during this study are included in this article; the data set used or analyzed during the current study are available from the corresponding author on reasonable request.

Supporting Information

The Supporting Information is available free of charge at https://pubs.acs.org/doi/10.1021/acsomega.3c05443.

Figure S1: process flow diagram for removal of Hg and SO_3 by dry flue gas adsorption; Figure S2: effect of H_2O on SO_2 removal efficiency of ZnS (PDF)

■ AUTHOR INFORMATION

Corresponding Author

Songjian Zhao − *School of Resources and Environmental Engineering, Jiangsu University of Technology, Changzhou, Jiangsu 213001, PR China;* orcid.org/0000-0001-8996-054X; Email: zhaosongjian@jsut.edu.cn

Authors

Wei Liu − *Jiangsu Environmental Engineering Technology Co. Ltd., Nanjing, Jiangsu 210019, China; Jiangsu Provincial Environmental Protection Group Co. Ltd., Nanjing, Jiangsu 210036, China; Jiangsu Province Engineering Research Center of Standardized Construction and Intelligent Management of Industrial Parks, Nanjing, Jiangsu 210019, China*

Xin Min − *School of Resources and Environmental Engineering, Jiangsu University of Technology, Changzhou, Jiangsu 213001, PR China*

Jin Zhao − *School of Resources and Environmental Engineering, Jiangsu University of Technology, Changzhou, Jiangsu 213001, PR China*

Complete contact information is available at: https://pubs.acs.org/10.1021/acsomega.3c05443

Table 4. Results after Adding Compound Absorbent

position	SO_3 (ppm)	Hg^{2+} ($\mu g/m^3$)	Hg^0 ($\mu g/m^3$)	total Hg ($\mu g/m^3$)
system import	3111 ± 122	488.0 ± 60.3	553.2 ± 98.2	1041.2 ± 158.5
cyclone dust collector outlet	2326 ± 68.9			
bag filter outlet	2097 ± 79.8	460.7 ± 60.7	130.8 ± 47.7	591.3 ± 13.0
removal efficiency %	32.6	5.6	76.3	43.2

https://doi.org/10.1021/acsomega.3c05443
ACS Omega 2023, 8, 42741−42747

Author Contributions

[#]W.L. and X.M. contributed equally to this work. The manuscript was reviewed and ethical approved for publication by all authors. The manuscript was reviewed and consents to participate by all authors. The manuscript was reviewed and consents to publish by all authors. W.L.: experiment, materials characterization analysis, writing; X.M.: experiments, materials synthesis, writing; J.Z.: materials characterization, materials synthesis; S.Z.: conceptualization, methodology, reviewing and editing.

Funding

This work was partly supported by the Science and Technology Planning Project of Jiangsu Provincial Environmental Protection Group(No. JSEP-TZ-2022−2003-RE). Supported by the Foundation Research Project of Jiangsu Province the Natural Science Fund (No. BK20210983).

Notes

The authors declare no competing financial interest.

REFERENCES

(1) Xu, J.; Li, Y.; Wang, S.; Long, S.; Wu, Y.; Chen, Z. Sources, transfers and the fate of heavy metals in soil-wheat systems: The case of lead (Pb)/zinc (Zn) smelting region. *J. Hazard. Mater.* **2023**, *441*, No. 129863.

(2) Li, P. Z.; Lin, C. Y.; Cheng, H. G.; Duan, X. L.; Lei, K. Contamination and health risks of soil heavy metals around a lead/zinc smelter in southwestern China. *Ecotoxicol. Environ. Safety* **2015**, *113*, 391−399.

(3) Lee, P. K.; Kang, M. J.; Jeong, Y. J.; Kwon, Y. K.; Yu, S. Lead isotopes combined with geochemical and mineralogical analyses for source identification of arsenic in agricultural soils surrounding a zinc smelter. *J. Hazard. Mater.* **2020**, *382*, No. 121044.

(4) Xie, X. F.; Zhang, Z. H.; Chen, Z. K.; Wu, J. Y.; Li, Z. L.; Zhong, S. P.; Liu, H.; Xu, Z. F.; Zhilou, L. In-situ preparation of zinc sulfide adsorbent using local materials for elemental mercury immobilization and recovery from zinc smelting flue gas. *Chem. Eng. J.* **2022**, *429*, No. 132115.

(5) Khalil, A. T. A.; Buddin, M. M. H. S.; Puasa, S. W.; Ahmad, A. L. Reuse of waste cooking oil (WCO) as diluent in green emulsion liquid membrane (GELM) for zinc extraction *Environ. Sci. Pollut. Res. Int.* 2023, *30*, 45244−45258, DOI: 10.1007/s11356-023-25208-0.

(6) Jiang, T.; Wang, P. C.; Zhang, T.; Zhu, D. Q.; Liu, Z. H. A novel solvent extraction system to recover germanium from H_2SO_4 leaching liquor of secondary zinc oxide: Extraction behavior and mechanism. *J. Cleaner Prod.* **2023**, *383*, No. 135399.

(7) Anirudhan, T. S.; Shainy, F. Effective removal of mercury(II) ions from chlor-alkali industrial wastewater using 2-mercaptobenzamide modified itaconic acid-grafted-magnetite nanocellulose composite. *J. Colloid Interface Sci.* **2015**, *456*, 22−31.

(8) Suess, E.; Berg, M.; Bouchet, S.; Cayo, L.; Hug, S. J.; Kaegi, R.; Voegelin, A.; Winkel, L. H. E.; Tessier, E.; Amouroux, D.; Buser, A. M. Mercury loads and fluxes from wastewater: A nationwide survey in Switzerland. *Water Res.* **2020**, *175*, No. 115708.

(9) Habashi, F. Metallurgical Plants - How Mercury Pollution Is Abated. *Environ. Sci. Technol.* **1978**, *12* (13), 1372−1376.

(10) Luo, Q.; Ren, Y. X.; Sun, Z. H.; Li, Y.; Li, B.; Yang, S.; Zhang, W. P.; Hu, Y. N.; Cheng, H. F. Atmospheric mercury pollution caused by fluorescent lamp manufacturing and the associated human health risk in a large industrial and commercial city. *Environ. Pollut.* **2021**, *269*, No. 116146.

(11) Yang, J. C.; Su, J. C.; Chen, L.; Huang, Y.; Gao, M. K.; Zhang, M. K.; Yang, M. T.; Zhang, X.; Wang, F. M.; Shen, B. X. Mercury removal using various modified V/Ti-based SCR catalysts: A review. *J. Hazard. Mater.* **2022**, *436*, No. 129115.

(12) Ishag, A.; Yue, Y. X.; Xiao, J. T.; Huang, X. S.; Sun, Y. B. Recent advances on the adsorption and oxidation of mercury from coal-fired flue gas: A review. *J. Cleaner Prod.* **2022**, *367*, No. 133111.

(13) Zhang, H. C.; Wang, T.; Zhang, Y. S.; Wang, J. W.; Sun, B. M.; Pan, W. P. A review on adsorbent/catalyst application for mercury removal in flue gas: Effect of sulphur oxides (SO_2, SO_3). *J. Cleaner Prod.* **2020**, *276*, No. 124220.

(14) Ma, Y. P.; Mu, B. L.; Zhang, X. J.; Xu, H. M.; Qu, Z.; Gao, L.; Li, B.; Tian, J. J. Ag-Fe_3O_4@rGO ternary magnetic adsorbent for gaseous elemental mercury removal from coal-fired flue gas. *Fuel* **2019**, *239*, 579−586.

(15) Yang, W.; Chen, H.; Han, X.; Ding, S.; Shan, Y.; Liu, Y. X. Preparation of magnetic Co-Fe modified porous carbon from agricultural wastes by microwave and steam activation for mercury removal. *J. Hazard. Mater.* **2020**, *381*, No. 120981.

(16) Yang, J. P.; Zhao, Y. C.; Ma, S. M.; Zhu, B. B.; Zhang, J. Y.; Zheng, C. G. Mercury Removal by Magnetic Biochar Derived from Simultaneous Activation and Magnetization of Sawdust. *Environ. Sci. Technol.* **2016**, *50* (21), 12040−12047.

(17) Liu, X.; Gao, Z.; Wang, C.; Zhao, M.; Ding, X.; Yang, W.; Ding, Z. Hg0 oxidation and SO3, Pb0, PbO, PbCl2 and As2O3 adsorption by graphene-based bimetallic catalyst ((Fe,Co)@N-GN): A DFT study. *Appl. Surf. Sci.* **2019**, *496*, No. 143686.

(18) Liao, Y.; Xu, H.; Liu, W.; Ni, H.; Zhang, X.; Zhai, A.; Quan, Z.; Qu, Z.; Yan, N. One Step Interface Activation of ZnS Using Cupric Ions for Mercury Recovery from Nonferrous Smelting Flue Gas. *Environ. Sci. Technol.* **2019**, *53* (8), 4511−4518.

(19) Liao, Y.; Liu, W.; Xu, H.; Hong, Q.; Wang, Y.; Qu, Z.; Yan, N. Zinc concentrate internal circulation technology for elemental mercury recovery from zinc smelting flue gas. *Fuel* **2020**, *280*, No. 118566.

(20) Liu, W.; Xu, H. M.; Liao, Y.; Quan, Z. W.; Li, S. C.; Zhao, S. J.; Qu, Z.; Yan, N. Q. Recyclable CuS sorbent with large mercury adsorption capacity in the presence of SO_2 from non-ferrous metal smelting flue gas. *Fuel* **2019**, *235*, 847−854.

(21) Pang, X.; Liu, W.; Xu, H.; Hong, Q.; Cui, P.; Huang, W.; Qu, Z.; Yan, N. Selective uptake of gaseous sulfur trioxide and mercury in ZnO-CuS composite at elevated temperatures from SO2-rich flue gas. *Chem. Eng. J.* **2022**, *427*, No. 132035.

(22) Zheng, C. H.; Wang, Y. F.; Liu, Y.; Yang, Z. D.; Qu, R. Y.; Ye, D.; Liang, C. S.; Liu, S. J.; Gao, X. Formation, transformation, measurement, and control of SO3 in coal-fired power plants. *Fuel* **2019**, *241*, 327−346.

https://doi.org/10.1021/acsomega.3c05443
ACS Omega 2023, 8, 42741−42747